Different Aspects of Geometrical Optimization for Compact Heat Exchangers

RAMIN RAHMANI[a], IRAJ MIRZAEE[b], AHAD RAMEZANPOUR[a], HASSAN SHIRVANI[a]
[a] Faculty of Science and Technology, Anglia Ruskin University,
Victoria Road South, Chelmsford, Essex CM1 1LL, UK
[b] Department of Mechanical Engineering, Faculty of Engineering,
Urmia University, Urmia, Iran
Email: r.rahmani@anglia.ac.uk

Abstract: In this study a two dimensional, steady state and incompressible laminar flow for staggered tube arrays in crossflow is investigated numerically. The study is based on a patented (APU, UK May 2001) compact heat exchanger design using implanted vortex generators on the internal flow, and change of fluid momentum in a turbulent jet on the external flow side. A finite-volume method is used to discretize and solve the governing equations for the geometries expressed by a boundary-fitted coordinate system. Solutions for the Reynolds numbers from 20 to 200 are obtained for a tube bundle with 10 longitudinal rows in different tube arrangements of ES, ET, and RS each with nominal pitch-to-diameter ratios of 1.33, 1.60 and 2.00. Different performance parameters which are used commonly to compare different heat exchangers are investigated and the performance parameters which account for pressure losses as well as occupied area are defined. The variations of these parameters with inlet Reynolds number and different nominal pitch-to-diameter ratios for different tube arrangements are also indicated. The optimum tube layouts for the studied flow and geometry ranges are shown as well.

Key-words: crossflow, laminar, staggered, tube bundle, efficiency, performance

1. Introduction

There are a lot of researches in the field of compact heat exchangers – including cooling of electronic circuits and devices – which are focused onto finding the optimum tube arrangement(s) for a given heat exchanger and/or proper using of augmented devices to increase the amount of heat transfer while the pressure head losses are minimized. In the absence of embedded devices such as vortex generators, the short length tubes in crossflow themselves can act as a vortex generator to improve the heat transfer in a compact heat exchanger. This study is based on a patented [1] compact heat exchanger design which uses this idea. To choose the optimal heat exchanger amongst many design options, including the patented compact heat exchanger using implanted vortex generators and impinging jets (see Fig. 1) [1] designer needs to have a large database available. The simulation approach is a mathematical model, which normally gives a good insight into understanding the flow and heat transfer for very limited cases. The simulation approach is a mathematical model, which normally gives a good insight in understanding the flow and heat transfer for very limited cases.

Literature review shows that different authors have used different parameters for comparison of the compact heat exchangers. For example; overall average friction factor [2-9] and pumping power [7-10] are used to show the frictional losses. There are also two major parameters to compare heat transfer characteristics of different models: average Nusselt number [6-9] and the overall heat transfer rate from tube bank [6, 11]. Some resources have defined some parameters as a combination of the aforementioned parameters to compare different tube bundles to find out the most efficient one. Therefore different parameters are used to show the performance (or efficiency) of different types of heat exchangers mostly include fins. Uzol and Camci in [2] and [3] have used a parameter named specific friction loss in their works. This parameter is constructed using calculated average Nusselt number and average friction factor. Yun and Lee [4] have used the JF factor which is the ratio of computed Colburn *j*-factor and friction factor. Horvat and Catton in [5] and [6] have used the ratio of the total heat transfer rate from the tube bundle to the required pumping power as a parameter to compare the performance of different cases. It seems there is lack of works on finding the optimal tube distances and/or tube arrangements for compact heat exchangers in numerical analyses field.

Bejan uses different approaches to find the optimal spacing between tubes in a compact heat exchanger. Bejan *et al.* in [7], theoretically, numerically and experimentally studied how to select the spacing between horizontal cylinders in an array with laminar natural convection, such that the total heat transfer between the array and the ambient is maximized. They recommended some correlations for this aim and conclude that the optimal spacing is relatively insensitive to whether the cylinders are isothermal or with uniform heat flux. Furthermore he in [8] similar to [9] theoretically investigated, by the concept of scale analysis [10], the optimal spacing of cylinders in crossflow forced convection. He showed that the optimal spacing can be predicted based on a simple theory, so called the method of intersecting of asymptotes, and the ratio of optimum spacing to cylinder diameter is not a constant. In [11], Stanescu *et al.* continued [7] to forced convection. They considered a bundle of circular tubes with different spaces and Reynolds numbers. They theoretically showed that there is an optimum space between tubes (or pin fins). Moreover, they showed that the optimal spacing decreases as the free-stream velocity (or inlet Reynolds number) increases, and as the flow length of the array decreases. In [12] Fowler *et al*. continued their works in [11] and [7] to staggered plates in forced convection. They did the similar investigations on the plates.

In this study it was attempted to investigate some tube bundle performance parameters for several staggered tube arrangements at different nominal pitch-to-diameter ratios when cooling flow passes with different inlet Reynolds numbers through tubes. It is attended, from the definition of performance parameters, to achieve a model which has the highest heat transfer rate while produces lowest or at least lower pressure drops in a rational range. Some parameters are defined to evaluate the bundle performance which will be considered here.

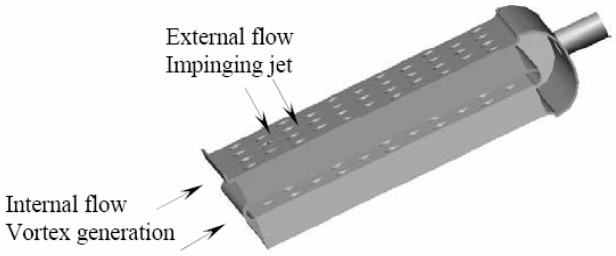

Figure 1. 2001 APU patented heat exchanger with implanted vortex generators and impinging jet

Furthermore, it should be noted that in some cases we may need to have a model with highest heat transfer rate and the space (volume) limitations are more considerable than pressure losses. This is true for confined heat exchanger with application in spacecraft or electronic cooling purposes. In these situations there must be a balance between pressure drops and occupied volume. Therefore, this type of performance evaluations is also considered here. To do this, three common staggered tube patterns in compact heat exchangers is selected: equal spacing (ES), equilateral triangle (ET), and rotated square (RS). These are shown in Fig. 2. Each of these patterns is considered at three different nominal pitch-to-diameter ratios of 1.33, 1.60 and 2.00.

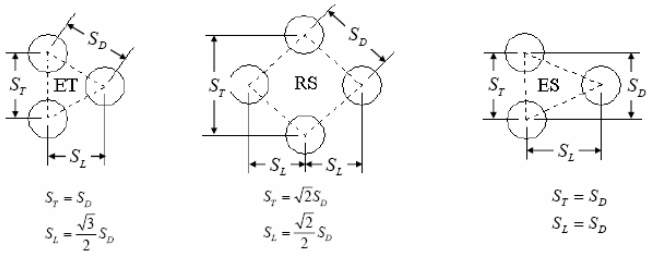

Figure 2. Tube arrangements

Table 1 gives a summary of transverse and longitudinal pitch-to-diameter ratios for the nominal pitch-to-diameter ratios of 1.33, 1.60, and 2.00 used for the three above different arrangements. It is also assumed that the passing fluid flows with inlet Reynolds number in the range of $20 \leq Re_{in} \leq 200$. This ensures that the laminar regime is dominated.

Table 1. Summary of pitch-to-diameter ratios

	ES		ET		RS	
S_D^*	S_T^*	S_L^*	S_T^*	S_L^*	S_T^*	S_L^*
1.33	1.33	1.33	1.33	1.1518	1.8809	0.9405
1.60	1.60	1.60	1.60	1.3854	2.2627	1.1314
2.00	2.00	2.00	2.00	1.7320	2.8284	1.4142

The results for the local values and variations of important flow and heat transfer parameters such as streamlines, isotherms, skin friction coefficient and local Nusselt number are recently investigated for the same geometries and Reynolds numbers by the authors [13-14]. In addition, the variations of some important parameters which are used here to define the performance parameters, have already been investigated and presented by authors [15-17]. For instance variations of friction factor (f_c), average Nusselt number (Nu_{LM}) and Colburn j factor with Reynolds number and nominal pitch-to-diameter ratio are shown in [15,16] or the variations of pumping power ($\dot{W}$)

and total heat transfer rate (q) are presented at [16,17]. In fact, this study is the continuation of the previous studies which mainly considers the performance parameters and their variations, i.e. the different performance parameters which will be discussed here are based on the aforementioned studied parameters.

2. Problem Description and Governing Equations

The convective heat transfer for fluid flow passing over the heated tube bundles with staggered tube arrangements is considered (see Fig. 3). The fluid flow is assumed to be two dimensional, steady, laminar and incompressible with constant properties. Due to the repeated condition in the y-direction, the solution domain is bounded by the inlet, the outlet, and by lines MN and KL as shown in Fig. 3. The MN and KL boundaries (top and bottom respectively) consist of arcs representing the solid surfaces of the tubes, and the symmetry planes where there are no tubes.

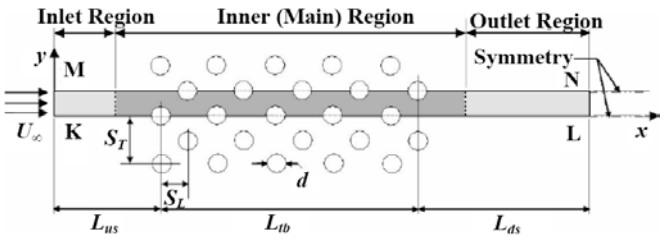

Figure 3. Staggered tube bank nomenclatures

The solution domain includes 10 longitudinal rows of tubes: 5 rows in top and 5 rows in bottom. The height of the solution domain is $S_T/2$. In order to decrease the effects of entrance and outlet regions, the dimensionless upstream and downstream lengths (L^*_{us} and L^*_{ds}, respectively) are assumed to be 5 and 40 respectively.

The governing equations for conservation of mass, and momentum in two dimensional Cartesian coordinate system, with the assumptions mentioned previously, can be written as follows:

$$\frac{\partial}{\partial x}(\rho u)+\frac{\partial}{\partial y}(\rho v)=0 \quad (1)$$

$$\frac{\partial}{\partial x}(\rho uu)+\frac{\partial}{\partial y}(\rho vu)=-\frac{\partial p}{\partial x}+\frac{\partial}{\partial x}\left(\mu\frac{\partial u}{\partial x}\right)+\frac{\partial}{\partial y}\left(\mu\frac{\partial u}{\partial y}\right) \quad (2)$$

$$\frac{\partial}{\partial x}(\rho uv)+\frac{\partial}{\partial y}(\rho vv)=-\frac{\partial p}{\partial y}+\frac{\partial}{\partial x}\left(\mu\frac{\partial v}{\partial x}\right)+\frac{\partial}{\partial y}\left(\mu\frac{\partial v}{\partial y}\right) \quad (3)$$

$$\frac{\partial}{\partial x}(\rho uc_pT)+\frac{\partial}{\partial y}(\rho vc_pT)=\frac{\partial}{\partial x}\left(k\frac{\partial T}{\partial x}\right)+\frac{\partial}{\partial y}\left(k\frac{\partial T}{\partial y}\right) \quad (4)$$

Equations (1)- (4) represent the conservation of mass, x- and y-direction momenta, and energy, respectively. The velocity components in the x- and y-directions (u and v), pressure (p), and temperature (T) are dependent variables.

Boundary conditions prescribed for these variables are summarized in Table 2.

Table 2. Summary of boundary conditions for u, v, and T

	u	v	T
Inlet ($x=0$)	$u=u_{in}$	$v=0$	$T=T_{in}$
Exit ($x=L_{us}+L_{tb}+L_{ds}$)	$\partial u/\partial x=0$	$v=0$	$\partial T/\partial x=0$
Symmetry	$\partial u/\partial y=0$	$v=0$	$\partial T/\partial y=0$
Tube Surface	$u=0$	$v=0$	$T=T_w$

3. Numerical Method and Grid Generation

A finite-volume method described by Patankar [18] with cooperation of the SIMPLE algorithm for pressure correction was applied to discretize and solve the governing equations. A first-order upwind scheme is employed for all scalar transport equations and the second-order damping scheme is used in the domains with high gradients of physical properties.

The computational domain was divided into three sub-domains: inlet domain, internal (or main) domain, and outlet domain, as shown in Fig. 3. The quadrilateral-shaped control volumes were obtained by generating an unstructured grid distribution on each domain.

The grid independence test was performed by changing the number of grids with different expansion and contraction factors. It was found that the more grid refinement does not affect considerably the results. Convergence was declared when the normalized maximum RMS (root mean square) values were less than 1×10^{-12} for u, v, and p and less than 1×10^{-15} for T.

The computational procedure was carried out for all possible combinations of arrangements, Reynolds numbers, and pitch-to-diameter ratios. The computational model is validated using available experimental data from Nishimura [19].

Figure 4 shows the variation of the skin-friction coefficient for ES arrangement with θ for Re_{in}=54 and S^*_D=2.0. As it can be seen, there is a good agreement between the computed results and experiment.

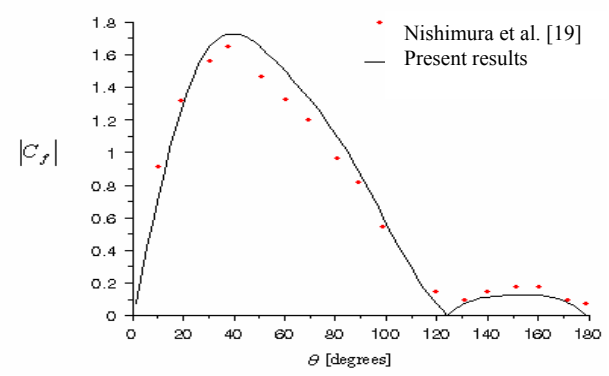

Figure 4. Comparison between the computed and experimental results in a bundle with an ES arrangement at Re_{in} =54 with S^*_D=2.0

4. Results and Discussion

In this section variations of a series of defined performance parameters with the geometrical parameter called dimensionless nominal pitch-to-diameter ratio will be presented in order to specify appropriated optimization parameters regarding to a particular demand. The graphs will be sketched to show the variations of these parameters versus nominal pitch-to-diameter ratio when arrangements as well as inlet Reynolds number differ.

4.1 Specific Nusselt Number (ε)

This is a parameter to compare the performance of different models used by Uzol and Camci in [2] and [3] considering both the heat transfer enhancement and the pressure loss characteristics at different Reynolds numbers. This parameter in [2] has been called the "specific friction loss" and is defined as

$$\varepsilon_f = \frac{f_c}{Nu_{av}} \tag{5}$$

This parameter basically is an indication of the pressure loss levels for each model in order to achieve same amount of heat transfer capability on the wall inside the wake. But at this study we have used the reverse ratio of this parameter and named it ε, the specific Nusselt number,

$$\varepsilon = \frac{Nu_{LM}}{f_c} \tag{6}$$

In the equations above, f_c is overall pressure drop factor or in other words average friction factor and is defined by equation below [13]

$$f_c = \frac{(p_{in} - p_{out})}{2\rho(V_{in})^2 N_L} \tag{7}$$

where N_L, the number of tube rows, was taken as 10.

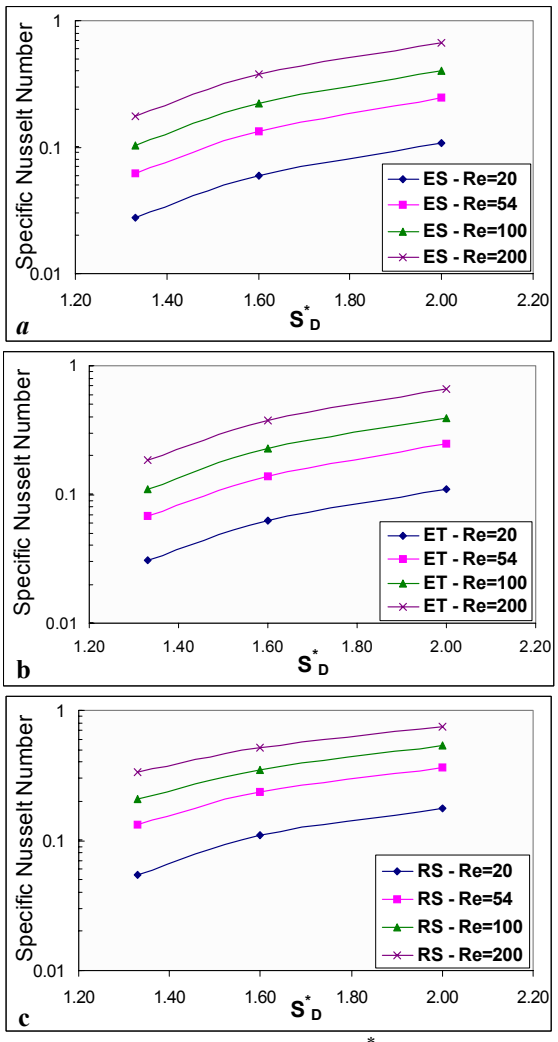

Figure 5. Variations of ε versus S^*_D for various inlet Reynolds numbers at different arrangements: (a) ES arrangement; (b) ET arrangement; (c) RS arrangement.

The average Nusselt number, Nu_{LM}, is based on the total rate of heat transfer and a log-mean temperature difference can be defined by [13]

$$Nu_{LM} = \frac{\bar{h}D}{k} = \frac{q}{A_s \Delta T_{LM}} \frac{D}{k} \tag{8}$$

where q is the total rate of heat transfer to the fluid and A_s is the total surface area of tubes exposed to the fluid in the solution domain. The log-mean temperature difference was defined by [13]

$$\Delta T_{LM} = \frac{(T_w - T_{in}) - (T_w - T_{out})}{\ln[(T_w - T_{in})/(T_w - T_{out})]} \quad (9)$$

The total heat transfer rate was calculated as either the integration of q''_w over all the tube surface area or as the total change in the fluid enthalpy between the inlet and the outlet.

The results are shown in Fig. 5. The values of both of Nu_{LM} and f_c decrease with increasing of nominal pitch-to-diameter ratio [15, 16]. However, their ratio shows a reverse trend here. Increasing of Reynolds number at the same nominal pitch increases the specific Nusselt number. The curves in this figure show that increasing of ε with S^*_D is linear especially for ES and ET arrangements which this line can be approximated by a linear equation. In addition, it can be observed that the RS arrangement has higher specific Nusselt number with respect to ES and ET arrangements which have almost conformal curves.

4.2 Tube Bundle Efficiency (λ)

The ratio of the total heat transfer rate from the tube bundle to the required pumping power is used to compare the performance of different models in some resources (e.g. [26] and [27]). This parameter which is called tube bundle efficiency is defined as: [17]

$$\lambda = \frac{q}{\dot{W}} = \frac{\rho.c_p(T_{out} - T_{in})}{\Delta p} \quad (10)$$

in which q is total heat transfer rate and was calculated as either the integration of q''_w over all the tube surface area or as the total change in the fluid enthalpy between the inlet and the outlet:

$$q = \dot{M}c_p\Delta T = \dot{M}c_p(T_{out} - T_{in}) \quad (11)$$

which

$$\dot{M} = \rho u_{in} A_c \quad (12)$$

and A_c is inlet cross sectional area of channel. $\dot{W}$ is pumping power and is defined as the production of volume flow rate and pressure loss:

$$\dot{W} = \dot{V}.\Delta p \quad (13)$$

where $\dot{V}$ is volume flow rate and is calculated as

$$\dot{V} = \frac{\dot{M}}{\rho} = u_{in}.A_c \quad (14)$$

in which u_{in} is the inlet velocity and A_c is the inlet cross-sectional area of the channel.

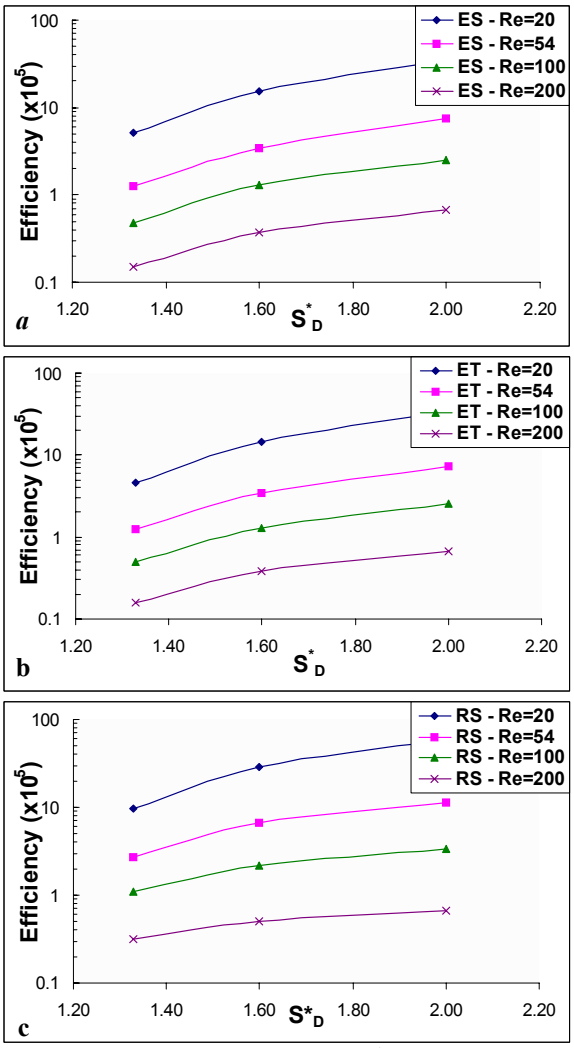

Figure 6. Variations of λ versus S^*_D for various inlet Reynolds numbers at different arrangements: (a) ES arrangement; (b) ET arrangement; (c) RS arrangement.

The resulted curves are presented in Fig 6. Studying of this parameter shows that in all arrangements, the throughflow with lower inlet Reynolds number produces higher efficiency, i.e. higher heat transfer rate with respect to needed pumping power. Moreover, the geometries with larger tube spaces (S^*_D) act better in comparison with geometries with smaller nominal pitch-to-diameter ratios particularly at the lower Reynolds numbers. Comparing the graphs in Fig. 6 also reveals that at different Reynolds numbers the ES and ET arrangements have the same efficiency and RS arrangement has highest except at Re_{in}=200 with S^*_D=2.00 in which, all three arrangement have approximately same magnitude.

4.3 The Specific Heat Transfer Rate (σ)

All of the performance factors defined here – which are almost a collection of all performance factors which are used in this field by different resources as well as some other parameters which are introduced here – consider just the heat transfer versus pressure losses and show the relative advantage of models to each other transferring maximum heat where the pressure drops are low.

As discussed previously, developing of technology has brought to need considering the volume which heat exchanger occupies and one of the serious challenges in heat exchangers design is to design a geometry which gives higher requested heat rejection with a rational pressure drops whilst the overall space occupied by the heat exchanger becomes minimum. Figure 7 shows the total occupied area by each of the arrangements at different pitches.

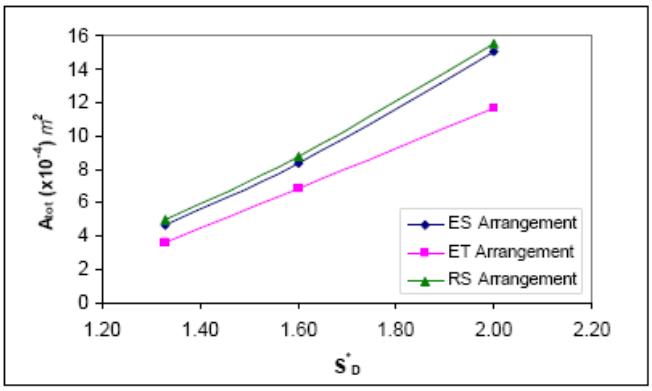

Figure 7. Variations of total occupied area by different arrangements at different investigated nominal pitch-to-diameter ratios

As it can be seen there is a considerable difference for the occupied areas by different arrangements even with the same nominal pitch-to-diameter ratios. For example RS arrangement has almost 37% more occupied area than ET arrangement at the same S^*_D of 2.00. [16] As it comes from [16], the ES and ET arrangements in the most of the cases have very near trends and values particularly at this study it has already seen that even their defined different performance factors are very near to each other while the curves in Fig. 7 show that at the same pitches ET arrangement has lower occupied area and from this viewpoint has advantages to ES arrangement.

In general, to investigate the occupied space effect of the models which were considered in this study, a parameter which defines the ratio of transferred heat to the volume (surface, in 2D) of model is defined here as:

$$\sigma = \frac{q}{V_{tot}\,(or A_{tot})} \tag{15}$$

in which V_{tot} is the total volume which is occupied by heat exchanger in three dimensional analyses and A_{tot} in two dimensional analyses. In Eq. (15), σ is specific heat transfer rate from whole of the tube bundle.

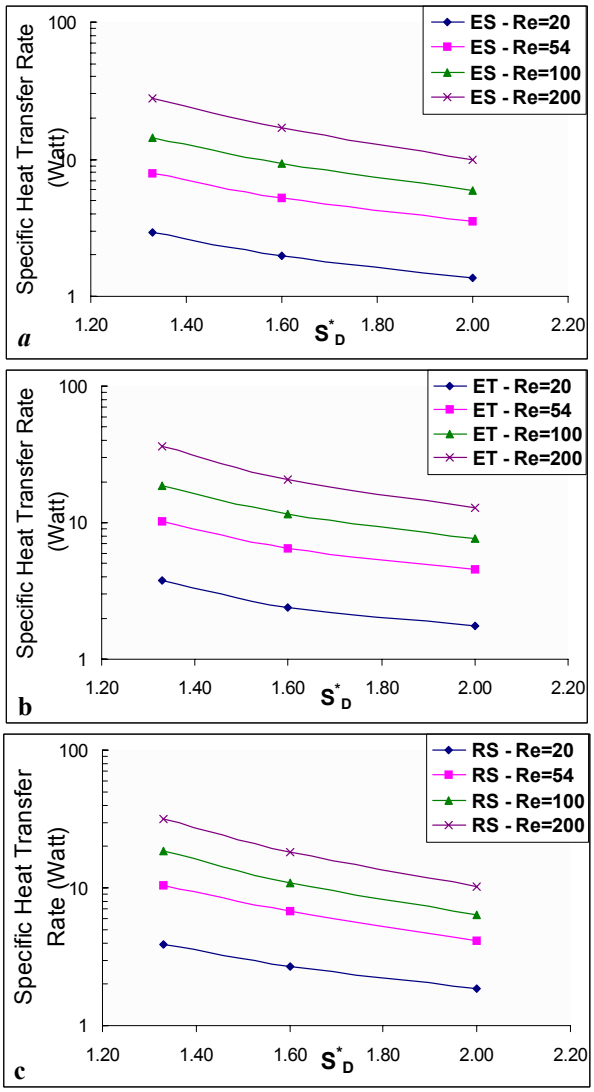

Figure 8. Variations of σ versus S^*_D for various inlet Reynolds numbers at different arrangements: (a) ES arrangement; (b) ET arrangement; (c) RS arrangement.

The results in Fig. 8 indicate that geometries with smaller nominal pitch-to-diameter ratios provide higher heat transfer per total area and as it can be expected throughflow with higher inlet Reynolds number will have higher rejected heat per total area. Comparing different arrangements at different Reynolds number in the graphs of Fig. 8 shows that ET and ES arrangements does not

have same values at the same pitches and ET arrangement shows higher σ than ES arrangement and in higher Reynolds numbers even has highest specific heat transfer rate. These graphs show that ES arrangement in all Reynolds numbers has lower σ magnitudes. However, the trend of curves illustrate that increasing of the Reynolds number reduces the σ values for RS arrangement and increasing the inlet Reynolds number may cause the curve for RS arrangement take lowest values.

4.4 The Overall Performance (ψ)

The overall performance of a tube bundle can be defined, by accounting for pressure losses and volume limitations as well as heat transfer from bundle. This parameter is defined in Eq. (16) as follows: [16]

$$\psi = \frac{\lambda}{A^*} \qquad (16)$$

in which λ is efficiency parameter defined by Eq. (10) and A^* is dimensionless area which is computed from dividing the total area occupied by bundle to the cross-sectional area of one of the tubes of bundle.

The parameter, ψ, defines the amount of transferred heat to the needed pumping power to the total occupied area (volume in 3D) by the geometry of the model. The graphs in Fig. 9 show that in all arrangements, when a flow with lower inlet Reynolds number passes through the channel produces higher overall efficiency and geometries with larger nominal pitch-to-diameter ratios, provide higher overall efficiency rather than geometries with smaller pitches except for RS arrangement at the some Reynolds numbers in which the overall efficiency reduces by increasing of the nominal pitch-to-diameter ratio.

Comparing of the overall performance of different arrangements at the same inlet Reynolds numbers indicates that in general RS arrangement in most of the pitches and inlet Reynolds numbers provides larger ψ values while ES arrangement has lowest ones (see Fig. 9). But by increasing of the Reynolds number of passing fluid flow, RS arrangement indicates a reduction in its overall performance especially at larger geometries. For example, RS arrangement at Re_{in}=200 and S^*_D=2.00 has minimum overall performance. However, the difference in the overall performance of ES and ET arrangements increases by increasing of the inlet Reynolds number.

If the variations of ψ curves versus S^*_D for RS arrangements at different inlet Reynolds numbers is followed through graphs of Fig. 9, it is illustrated that with increasing of Re_{in} causes the maximum point to move from the larger nominal pitch ratio to smaller one.

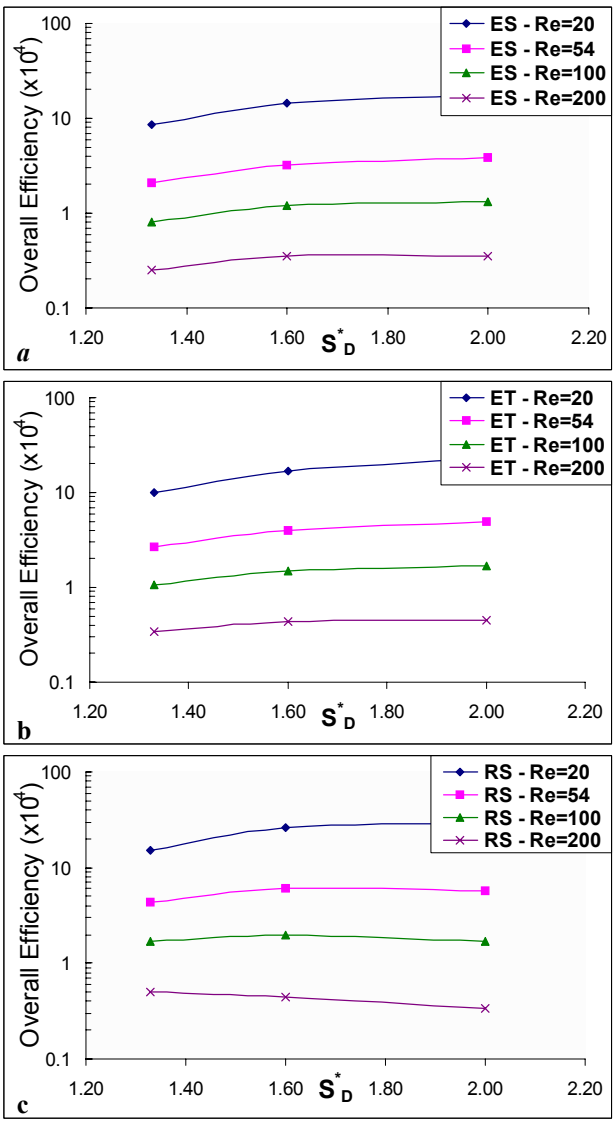

Figure 9. Variations of ψ versus S^*_D for various inlet Reynolds numbers at different arrangements: (a) ES arrangement; (b) ET arrangement; (c) RS arrangement.

5. Summary and Conclusions

The results show that the specific Nusselt number is higher for larger geometries with higher Reynolds number. The graphs for tube bundle efficiency (λ) which reflects the ratio of total heat transfer rate to the pumping power and can be a practical parameter indicated that the efficiency of the tube bundles will reduce if the Reynolds number of passing fluid becomes increased. But for larger geometries there is higher efficiency. This means that the flow with low Reynolds number passing through the larger geometry will produce higher efficiency and

the increasing of heat transfer due to increasing of the Reynolds number is not useful from the efficiency view point because in this regard, the pumping power will increase more than the amount of transferred heat. Therefore, the magnitude of efficiency will reduce. Another comparing may be done by considering the size of the tube bundles. At the same conditions the specific heat transfer rate for ET arrangement is highest while ES arrangement shows lowest σ and in all arrangements in all Reynolds numbers the smaller geometries show higher specific heat transfer rate. The results for overall performance which accounts for the effect of the size and pumping power indicated that the trend of curves is like to their correspondent for efficiency factor and the only difference is that at the same nominal pitch ET arrangement shows higher overall performance than ES arrangement while their efficiency is the same.

The results for variation of efficiency factor with respect to the nominal pitch show that for RS arrangement at higher Reynolds numbers (e.g. Re_{in}=200) the efficiency of the tube bundle does not increase considerably by enlargement the geometry more than S^*_D=1.60. In this regard increasing of Reynolds number from 20 to 200 for RS arrangement will produce a nominal pitch-to-diameter ratio which will have the highest overall performance in the range of S^*_D=1.33 up to 2.00.

Nomenclature:

A^*	dimensionless area ($=A_{tot}/A_c$)
A_c	inlet cross-sectional area of the channel [m^2]
A_s	surface of one tube [m^2]
A_{tot}	total surface area of tubes [m^2]
c_p	specific heat capacity [J/kgK]
D	tube diameter [m]
f_c	average friction factor
$\overline{h}$	average heat transfer coefficient [W/m^{2}K]
k	thermal conductivity [W/mK]
L_{ds}	downstream length [m] (Fig. 3)
L^*_{ds}	dimensionless downstream length ($=L_{ds}/D$)
L_{tb}	tube bank length [m] (Fig. 3)
L^*_{tb}	dimensionless tube bank length ($=L_{tb}/D$)
L_{us}	upstream length [m] (Fig. 3)
L^*_{us}	dimensionless upstream length ($=L_{us}/D$)
$\dot{M}$	mass flow rate [kg/s]
N_L	the number of tube rows
Nu_{av}	average Nusselt number
Nu_{LM}	average Nusselt number based on a log-mean temperature difference
p	pressure [Pa]
$\dot{V}$	volume flow rate [m^3/s]
q	total heat transfer rate [W]
q''_w	heat flux from tube walls [W/m^2]
Re_{in}	Reynolds number based on inlet velocity ($=u_{in}D/\nu$)
S_D	nominal pitch [m] (Fig. 2)
S^*_D	nominal pitch-to-diameter ratio ($=S_D/D$)
S_L	longitudinal pitch [m] (Fig. 2)
S^*_L	longitudinal pitch-to-diameter ratio ($=S_L/D$)
S_T	transverse pitch [m] (Fig. 2)
S^*_T	nominal pitch-to-diameter ratio ($=S_T/D$)
T	temperature [K]
u	x-direction velocity [m/s]
v	y-direction velocity [m/s]
u_{in}	inlet velocity [m/s]
V_{tot}	total volume of a tube bundle [m^3]
$\dot{W}$	pumping power [W]
x	Cartesian x-coordinate [m]
y	Cartesian y-coordinate [m]

Greek symbols

Δp	pressure difference [Pa]
ΔT	temperature difference [K]
ε	specific Nusselt number
ε_f	specific friction loss
θ	angle from the front of tube [degree]
λ	tube bundle efficiency
μ	fluid dynamic viscosity [kg/m.s]
ν	fluid cinematic viscosity [m^2/s] ($=\mu/\rho$)
ρ	fluid density [kg/m^3]
σ	specific heat transfer rate [W/m^2]
ψ	overall performance of tube bundle

Subscripts

in	inlet
out	outlet
w	tube wall

Abbreviations

ES	equal spacing
ET	equilateral triangle
RS	rotated square
RMS	root mean square

References:

[1] APU, UK, May 2001. Details have been published by the UK patent office.

[2] O. Uzol, C. Camci, Elliptical Pin Fins as an

Alternative to Circular Pin Fins for Gas Turbine Blade Cooling Applications. Part 1: Endwall Heat Transfer and Total Pressure Loss Characteristics, 2001, *URL:www.pcrsonal.psu.edu/faculty/c/x/cxc11/papers/camci_uzol_epf_01.pdf*.

[3] O. Uzol, C. Camci, Elliptical Pin Fins as an Alternative to Circular Pin Fins for Gas Turbine Blade Cooling Applications. Part 2: Wake Flow Field Measurements and Visualization Using Particle Image Velocimetry, 2001, *URL:www.pcrsonal.psu.edu/faculty/c/x/cxc11/papers/camci_uzol_epf_02.pdf*.

[4] J.-Y. Yun, K.-S. Lee, An Investigation on Heat Transfer Characteristics of Fin and Tube Heat Exchangers Using The Geometry Similitude Method, *J. of air-conditioning and refrigeration*, Vol. 5, 1997, pp. 57-67.

[5] A. Horvat, I. Catton, Modeling of Conjugate Heat Transfer Using Galerkin Approach, *URL: www.2.ijs.si/~ahorvat/publications/mchtugm.pdf*.

[6] A. Horvat, I. Catton, Numerical Technique for Modeling Conjugate Heat Transfer in an Electronic Device Heat Sink, *Int. J. Heat Mass Transfer*, Vol. 46, 2003, pp. 2155-2168.

[7] A. Bejan, A.-J. Fowler, G. Stanescu, The Optimal Spacing Between Horizontal Cylinders in a Fixed Volume Cooled by Natural Convection, *Int. J. Heat Transfer*, Vol. 38, 1995, pp. 2047-2055.

[8] A. Bejan, The Optimal Spacing for Cylinders in Crossflow Forced Convection, *ASME J. Heat Transfer*, Vol. 117, 1995, pp. 767-770.

[9] A. Bejan, A.-M. Morega, The Optimal Spacing of a Stack of Plates Cooled by Turbulent Forced Convection, *Int. J. Heat Mass Transfer*, Vol. 37, 1994, pp. 1045-1048.

[10] A. Bejan, *Convection Heat Transfer,* 1st Ed., John Wiley & Sons, New York, 1984.

[11] G. Stanescu, A.J. Fowler, and A. Bejan, The Optimal Spacing of Cylinders in Free-Stream Cross-Sectional Forced Convection, *Int. J. Heat Mass Transfer*, Vol. 39, 1996, pp. 311-317.

[12] A.-J. Fowler, G.-A. Ledezma, and A. Bejan, Optimal Geometric Arrangement of Staggered Plates in Forced Convection, *Int. J. Heat Mass Transfer*, Vol. 40, 1997, pp. 1795-1805.

[13] R. Rahmani, I. Mirzaee, and H. Shirvani, Computation of a Laminar Flow and Heat Transfer of Air for Staggered Tube Arrays in Cross-Flow, *Iranian Journal of Mechanical Engineering (English)*, Vol. 6(2), 2005, pp. 19-33.

[14] R. Rahmani, A. Ramezanpour, I. Mirzaee, and H. Shirvani, Computation of Velocity Profiles and Pressure Coefficients for a Laminar Flow of Air over Staggered Array of Tubes, *Proceedings of ASME's 2005 Summer Heat Transfer Conference,* July 17-22, 2005, San Francisco, CA, USA.

[15] R. Rahmani, I. Mirzaee, and H. Shirvani, The Optimized Pitch-to-Diameter Ratio for the Staggered Tube Arrays in Laminar Forced Convection, *Proceedings of 8th International and 12th Annual Mechanical Engineering Conference,* May 2004, Tarbiat Modarres University, Tehran, Iran.

[16] R. Rahmani, *An Investigation into Flat Plate Cooling with Staggered Implanted Vortex Generators*, Master Thesis, 2003, Urmia University, Iran.

[17] R. Rahmani, A. Ramezanpour, I. Mirzaee, and H. Shirvani, Design Optimization of Staggered Tube Arrays in Laminar Forced Convection, *In: R. Bennacer (Ed.), Progress in Computational Heat and Mass Transfer,* Lavoisier, Paris, 2005, pp. 850-855.

[18] S.-V. Patankar, *Numerical Heat Transfer and Fluid Flow,* Hemisphere Publishing, Washington, DC, 1980.

[19] T. Nishimura, *Flow across Tube Banks*, in: Cheremisinoff N.-P. (Ed.), Encyclopedia of Fluid Mechanics, Vol. 1, Gulf, Houston, TX, 1986, pp.763-78.